Article

Not peer-reviewed version

Comparative Analysis of the Human Proteome Profile in visceral Adipose Tissue and Liver Tissue in Individuals with Obesity With and Without MASLD and MASH

Julie Steen Pedersen *, Lili Niu, Nicolai Jacob Wever Albrechtsen, Viggo Bjerregaard Kristiansen, Inge Marie Poulsen, Reza Rafiolsadat Serizawa, Torben Hansen, Lise Lotte Gluud, Sten Madsbad, Flemming Bendtsen

Posted Date: 27 December 2024

doi: 10.20944/preprints202412.2367.v1

Keywords: MASLD; MASH; Untargeted proteomics; Liver tissue; Visceral adipose tissue; Obesity

 doi:10.20944/preprints202412.2367.v1

Article

Comparative Analysis of the Human Proteome Profile in visceral Adipose Tissue and Liver Tissue in Individuals with Obesity With and Without MASLD and MASH

Julie Steen Pedersen [1,*], Lili Niu [2], Nicolai J. Wever Albrechtsen [2,3,4], Viggo Bjerregaard Kristiansen [5], Inge Marie Poulsen [5], Reza Rafiolsadat Serizawa [4], Torben Hansen [6], Lise Lotte Gluud [1], Sten Madsbad [7,8] and Flemming Bendtsen [1,8]

[1] Gastrounit, Medical Division, Copenhagen University Hospital Hvidovre, Hvidovre, Copenhagen, Denmark
[2] NNF Center for Protein Research, Faculty of Health and Medical Sciences, University of Copenhagen, Copenhagen, Denmark
[3] Department of Clinical Medicine, University of Copenhagen, Copenhagen, Denmark
[4] Department of Clinical Biochemistry, Copenhagen University Hospital – Bispebjerg and Frederiksberg, Copenhagen, Denmark
[5] Gastrounit, Surgical Division, Copenhagen University Hospital Hvidovre, Hvidovre, Copenhagen, Denmark
[6] NNF Center for Basic Metabolic Research, Faculty of Health and Medical Sciences, University of Copenhagen, Copenhagen, Denmark
[7] Department of Endocrinology, Copenhagen University Hospital Hvidovre, Hvidovre, Copenhagen, Denmark
[8] Department of Clinical Medicine, Faculty of Health and Medical Sciences, University of Copenhagen, Denmark
* Correspondence: julie.steen.pedersen@regionh.dk

Abstract: Background/Objectives: Visceral adipose tissue (VAT) could be directly involved in the develop- ment of metabolic-associated steatotic liver disease (MASLD) and progression to metabolic-associated steatohepatitis (MASH). We employed untargeted proteomics analyses of paired VAT and liver biopsies to explore protein expression patterns in patients with obesity, MASLD and MASH in search of the potential presence of a MASH associated proteome in VAT and liver. **Methods**: VAT and liver tissue were collected from 70 subjects with severe obesity (SWO) and nine control study subjects without obesity (CON). SWO were stratified on the basis of liver histology into LS- (no liver steatosis), LS+ (liver steatosis) and MASH. Peptides were extracted from frozen tissue and were analyzed by liquid chromatography coupled to tandem mass spectrometry (LC-MS/MS). Raw files were analyzed with Spectronaut, proteins were searched against the human FASTA Uniprot database and the significantly expressed proteins in the two tissues were analyzed. P-values were false discovery rate (FDR) corrected. **Results**: 59 VAT and 42 liver proteins were significantly differentially expressed between the four groups; LS-, LS+ and MASH and CON. The majority were upregulated, and many were related to lipid metabolism. In VAT only one protein, SQOR, was significantly downregulated in the MASH group only. In liver tissue from patients with MASH six proteins were significantly altered compared with the three other groups. Correlation analyses between the top 10 positive VAT and liver proteins were dominated by inflammatory and detoxification proteins. **Conclusions**: Presence of MASH is not reflected in the VAT proteome and both the VAT, and the liver proteome are generally affected more by the presence of obesity than by MASLD severity.

 doi:10.20944/preprints202412.2367.v1

Several immunomodulating proteins correlated significantly between VAT and liver tissue and could reflect common pathophysiological characteristics.

Keywords: MASLD; MASH; Untargeted proteomics; Liver tissue; Visceral adipose tissue; Obesity

1. Introduction

The harmful impact of the excessive deposition of visceral adipose tissue (VAT) on risk of metabolic disease, type-2 diabetes (T2DM) and cardiovascular disease has been recognized for decades [1,2]Adipose tissue has major metabolic as well as endocrine functions. Adipose tissue derived adipocytokines and fat-derived metabolites such as free fatty acids affect the physiology of other organs [3–5] but VAT in particular is associated with metabolic disease risk. In clinical practice, waist circumference, which correlates with truncal VAT mass, is central to identifying patients at increased risk of metabolic comorbidities including metabolic associated steatotic liver disease (MASLD) and metabolic associated steatohepatitis (MASH)[6–8] An increased volume of visceral fat mass has a negative effect on the adipose tissue physiology and function as the subsequent increase in metabolic and oxidative load induce peripheral insulin resistance and act as stressors which alter the overall homeostasis of the VAT (ref). These alterations are exerted, in part, through changes in secretion of adipokines and proinflammatory cytokines with subsequent creation of an inflammatory and metabolic dysfunctional milieu with resultant adipocyte death and fibrosis deposition within the adipose tissue with infiltration and proliferation of macrophages contributing to obesity-associated adipose tissue inflammation [9–13]

In MASLD, triglycerides accumulate within the hepatocytes and cause liver steatosis; the condition may progress to MASH which is characterized by necroinflammation of the liver tissue and formation of liver fibrosis [14]. In MASLD, the changes that occur in VAT and liver tissue seem to share some pathophysiological characteristics. Mesenteric- and omental VAT are venously drained to the liver via the portal vein. According to the *portal vein theory*, free fatty acids adipocytokines and inflammatory cytokines derived from the VAT access the liver and could contribute to the development of liver steatosis and perhaps impact the progression of MASLD to MASH and liver fibrosis[15] .

Mass spectrometry (MS)-based proteomic analyses offer fast and large-scale analysis of the proteomes and can identify alterations in protein abundance in relation to disease. Therefore, MS-based proteomics could serve as a tool for identification of proteins that are up- or downregulated in patients with MASLD and MASH. The concomitant assessment of VAT and liver tissue allows for a detailed evaluation of the changes that occur in patients with mild, moderate or severe MASLD. Such analyses could provide important information about the underlying pathophysiology of MASLD.

As for MASLD, liver tissue proteomics has been successfully applied with focus on MASH associated hepatocarcinogenesis [16]and MASH fibrosis [17]. Additionally, our group has previously identified plasma biomarker candidates related to MASLD [18]. Consequently, it is of interest to perform detailed investigations of VAT in relation to MASLD.

In this cross-sectional study, we performed tissue proteomics analysis of paired omental VAT and liver tissue biopsies in 70 patients with severe obesity (SWO) without and with different stages of MASLD, as well as in nine control study subjects without obesity. We aimed to investigate a possible overlap of proteins that are simultaneously significantly up-or downregulated in both liver tissue and VAT and identify a potential MASH-specific proteome signature in both liver and VAT.

2. Materials and Methods

Cohort and Study Investigations

 doi:10.20944/preprints202412.2367.v1

We collected omental VAT and liver tissue from 70 SWO undergoing laparoscopic bariatric surgery and control study subjects without obesity (CON) undergoing planned laparoscopic cholecystectomy at Copenhagen University Hospital Hvidovre between December 2016 and October 2019. Tissue samples were collected immediately after induction of anesthesia and trocar placement, before the actual surgical procedure.

After sampling, the VAT was trimmed and cut into smaller pieces of 50-100 mg and immediately snap frozen in liquid nitrogen before storage in a -80-degree freezer until analysis. Liver tissue was similarly trimmed, capsule removed, and was cut into pieces of 50 mg, snap frozen and stored as described above. In addition, part of the liver biopsy underwent fixation in paraformaldehyde for later paraffin embedment and histological analysis.

The study was conducted according to the Declaration of Helsinki and was approved by the Regional Ethics Committee of Capital Region, Denmark (H-16030784 and H-16020782). All study subjects gave oral and written consent.

Liver histology and Grouping of Study Subjects

Liver histology was assessed by three pathologists. MASLD activity score the (referred to as the NAFLD activity score, NAS) was used to group patients with obesity as

1) No Liver steatosis (LS-): no liver steatosis present in liver biopsies
2) Liver steatosis present (LS+): Liver steatosis present but without MASH (NAS score < 5)
3) MASH: NAS ≥ 5 with points from all subcategories (steatosis, inflammation, and ballooning).

Sample Preparation for MS Analysis

Frozen liver and VAT biopsies were homogenized on a Precellys24 homogenizer (Bertin Technologies, France) in 300 µl SDC reduction and alkylation buffer (PreOmics GmbH, Martinsried, Germany) containing 1x Roche phosphatase inhibitor with ceramic beads (2.8 and 1.4mm zirconium oxide beads, Precellys). Approximately 15 mg of liver and 50 mg of VAT were processed as the starting material. Homogenates were incubated at 95 °C for 10 min (1200 rpm) and subsequently transferred to a new 1.5 ml Eppendorf tube, from which 45 µl of homogenate was further transferred to a 96-well plate and sonicated for 5 min using the Covaris Adaptive Focused Acoustics (AFA) sonication system (Covaris, USA). Protein content was determined by Tryptophan assay and an aliquot of 50 µg was digested overnight with LysC and trypsin in a 1:50 ratio (µg of enzyme to µg of protein) at 37 °C (1700 rpm). Peptides were acidified to a final concentration of 0.1% trifluoroacetic acid (TFA). Approximately 20 µg of peptides were loaded on Stage-Tips, washed with isopropanol/1% TFA (200µl) and then 0.2% TFA (200µl). Peptides were eluted with 60µl of elution buffer (80% acetonitrile/1% ammonia) and dried at 60°C using a SpeedVac centrifuge (Eppendorf, Concentrator plus). Dried peptides were dissolved and sonicated in 5% acetonitrile/0.1% TFA and concentration measured using Nanodrop. Peptide mixtures were stored at -80 °C until further analysis. Quality control samples of pooled tissue homogenate was included for measuring the workflow variation.

LC-MS/MS Analysis (Liquid Chromatography-Mass Spectroscopy/Mass Spectrometry Analysis)

Samples were measured using LC-MS instrumentation consisting of an EASY-nLC 1200 system (Thermo Fisher Scientific, San Jose, CA) interfaced on-line with a Q Exactive HF-X Orbitrap (Thermo Fisher Scientific, Bremen, Germany). Purified peptides were separated on 42.5 cm HPLC-columns (ID: 75 µm; in-house packed into the tip with ReproSil-Pur C18-AQ 1.9 µm resin (Dr. Maisch GmbH)). Approximately 500 ng of peptides were injected for each LC-MS/MS analysis. Peptides were loaded in buffer A (0.1% formic acid) and eluted with a linear 82 min gradient of 3-23% of buffer B (0.1% formic acid, 80% (v/v) acetonitrile), followed by an 8 min increase to 40% of buffer B. The gradients then increased to 98% of buffer B within 6 min, which was kept for 4 min. Flow rates were kept at 350

 doi:10.20944/preprints202412.2367.v1

nl/min. Re-equilibration was done for 4 µl of 0.1% buffer A at a pressure of 700 bar. Column temperature was kept at 60 °C.

For liver tissue samples, MS spectra were acquired using data-independent acquisition (DIA) mode, enabled by MaxQuant.Live [19] in which the scan protocol was defined. Each acquisition cycle consisted of a survey scan at resolution of 60,000 with an automatic gain control target (AGC) of 3e6, maximum injection time of 100 ms, followed by 66 DIA cycles at resolution of 15,000 with an AGC of 3e6/22ms IT at range 300-1,650 m/z). HCD fragmentation was set to normalized collision energy of 27%. In all scans, PhiSDM [20]was enabled with 100 iterations, spectra type was set to centroid. For adipose tissue samples, the DIA-MS method consisted of an MS1 scan from 350-1,650 m/z range (AGC target of 3e6, maximum injection time of 60 ms) at a resolution of 60,000 and 32 DIA segments (Dataset EV1 , AGC target of 3 x106, maximum injection time of 45 ms). The acquisition of samples was randomized to avoid bias.

Quantification and Statistical Analysis: Raw Data Processing and Analysis

All raw files were analyzed with Spectronaut Pulsar X (version 13.10) with default settings except that "Quantification" data filtering parameter "Q-value" was set to "complete". DIA hybrid spectra were searched against in-house generated libraries for human liver and adipose tissue using the same LC setup searching against human FASTA Uniprot database (version 201801, containing 93k entries). Proteins with more than 30% of missing values were discarded. Samples with less than 2,500 proteins quantified were also discarded. Normalization based on median protein intensity of each sample was performed. Remaining missing values of the dataset were imputed by drawing random samples from a normal distribution (down-shifted mean by 1.8 standard deviation (SD) and scaled SD (0.3) relative to that of proteome abundance distribution, with which we performed the statistical analysis. Statistical and bioinformatics analysis were performed with the Perseus software (version 1.6.5.0) and Python software. Specifically, one-way ANOVA was performed using the Python open-source statistical package 'pingouin' (https://pingouin-stats.org/) corrected for multiple hypothesis testing by Benjamini-Hochberg at 5% FDR (false discovery rate), followed by Tukey's HSD (honestly significant difference) test. Pair-wise correlation between VAT and liver tissue protein levels was performed with the pingouin.pairwise_corr module with a significance level of Benjamini-Hochberg corrected FDR at 5%.

Before filtering for 70 % (meaning that a given protein must be expressed/detectable in 70% of the samples within the specific tissue type) we detected 3200 protein groups (17570 peptides) in VAT and 5151 protein groups in liver tissue (35965 peptides).

The following databases were used to characterize function, cellular compartment and tissue distribution/expression of the significant proteins: Uniprot.org, proteinatlas.org, metabolicatlas.org, genecards.org and omim.org.

Illustrations were made in Perseus software and with use of biorender.com.

See *Figure 1* for schematic overview of the study workflow.

 doi:10.20944/preprints202412.2367.v1

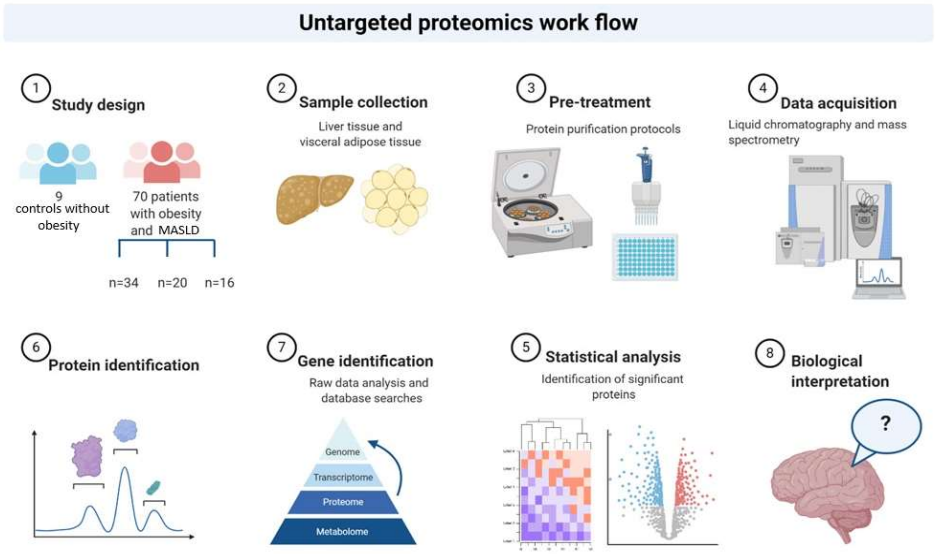

Figure 1. Schematic overview of study workflow.

3. Results

Table 1 depicts the clinical characteristics of the three MASLD groups (LS- n= 34, LS+ n=20, MASH n=16) and controls (CON n= 9). The number of patients with T2DM in each group was three (LS-), seven (LS+) and nine (MASH), respectively. Insulin resistance evaluated by HOMA-IR was progressively worsened from CON to MASH of about 4-fold. In the MASLD groups the BMI ranged from 41.8 - 44.6 kg/m² compared with 24.4 kg/m² the CON group.

Table 1. Clinical, anthropometrical, and biochemical data at baseline in study subjects with obesity undergoing bariatric surgery and stratified by MASLD severity and control study subjects without obesity.

	Subjects with obesity according to histology			
	LS- (n=34)	**LS+ (n=20)**	**MASH (n=16)**	**CON (n=9)**
Liver histology				
MASLD activity score (NAS)	2,3 (0,9)	3,2 (0,7)	5,1 (0,3)	1,1 (0,9)
Steatosis	0,0 (0,0)	1,1 (0,3)	1,7 (0,6)	0,0 (0,0)
Inflammation	1,1 (0,6)	0,9 (0,3)	1,6 (0,5)	0,9 (0,6)
Ballooning	1,2 (0,5)	1,2 (0,5)	1,9 (0,3)	0,2 (0,4)
Fibrosis	1,0 (0,3)	1,2 (0,4)	1,1 (0,5)	0,9 (0,3)
Age, years	45 (11)	45 (8)	45 (9)	39 (8)
Female (%)	25 (58)	9 (21)	9 (21)	7 (78)
Diabetes, n (%)	3 (16)	7 (37)	9 (47)	NA
Weight, kg	124 (20)*	138 (29)*	125 (17)*	71 (10)
BMI, kg/m²	41,8 (5,1)*	44,6 (8,4)*	42,4 (5,4)*	24,4 (2,2)
Waist-hip ratio	0,88 (0,11)	0,95 (0,13)	0,98 (0,08)*†	0,83 (0,10)
Systolic blood pressure, mmHg	126 (12)	130 (14)	131 (16)	117 (11)

 doi:10.20944/preprints202412.2367.v1

Diastolic Blood Pressure,mmHg	81(8)	82 (9)	82 (11)	77 (9)
Heart rate (BPM)	72 (12)	76 (13)	76 (14)	69 (7)
ALT, U/L	28 (10)	34 (15)	39 (15)*†	21 (9)
AST, U/L	24 (6)	25 (9)	27 (7)	21 (4)
Fasting plasma glucose, mmol/L	5,9 (0,7)	6,8 (1,5)	7,0 (2,2)	5,5 (0,4)
C-peptide pmol/L	1162 (343)*	1217 (257)*	1649 (523)*†§	791 (204)
Fasting insulin pmol/L	118,8 (47,3)	122,78 (44,6)	208,6 (88,9)*†§	63,3 (30,4)
HbA1c	35 (3)	41 (8)*†	37 (4)*	32 (3)
HOMA-IR	4,4 (1,8)	5,2 (1,7)	9,1 (4,2)*†§	2,2 (1,1)
LDL cholesterol, mmol/L	2,79 (0,98)	2,25 (0,56)	2,02 (0,61)	2,59 (0,53)
HDL cholesterol, mmol/L	1,22 (0,27)	1,20 (0,41)	1,09 (0,15)	1,39 (0,23)
VLDL cholesterol, mmol/L	0,58 (0,24)	0,69 (0,43)	0,75 (0,33)	0,50 (0,21)
Triglycerides, mmol/L	1,29 (0,52)	1,53 (0,95)	1,66 (0,74)	1,13 (0,50)
HsCRP (mg/L)	5,2 (4,1)	9,2 (10,7)*	5,1 (3,7)	1,5 (1,3)

Data are presented as mean (SD). P-values are one-way ANOVA with Bonferroni correction. or Chi Square/Fischer's exact test.

LS, liver steatosis; MASH, Metabolic associated steatohepatitis; CON, control study subjects; MASLD, Metabolic associated steatotic liver disease; RYGB, Roux-en-Y gastric bypass; SG, Sleeve gastrectomy; PCO, Polycystic ovarian syndrome; BMI, Body mass index; mmHg, Millimeter mercury; BPM, beats per minute; ALT, Alanine aminotransferase; AST, Aspartate aminotransferase; HbA1c, Glycated hemoglobin; HOMA-IR,

Homeostatic Model Assessment for Insulin Resistance; LDL, Low-density lipoprotein; HDL, High density lipoprotein; VLDL, Very low-density lipoprotein; HsCRP, Highly sensitive C-reactive protein mm, Millimeters.

*$P < 0.05$ compared with CON

†$P < 0.05$ compared with LS-

§ $P < 0.05$ compared with LS+

‡ $P < 0.05$ compared with MASH

3.1.1. Liver Tissue

In liver tissue we detected 32 differentially expressed proteins (DEPs) with significant up-or downregulation between the four groups *(Table 2 and Figure 2)*. Of these, 18 were upregulated, and 14 were downregulated in the MASLD groups when compared to CON.

 doi:10.20944/preprints202412.2367.v1

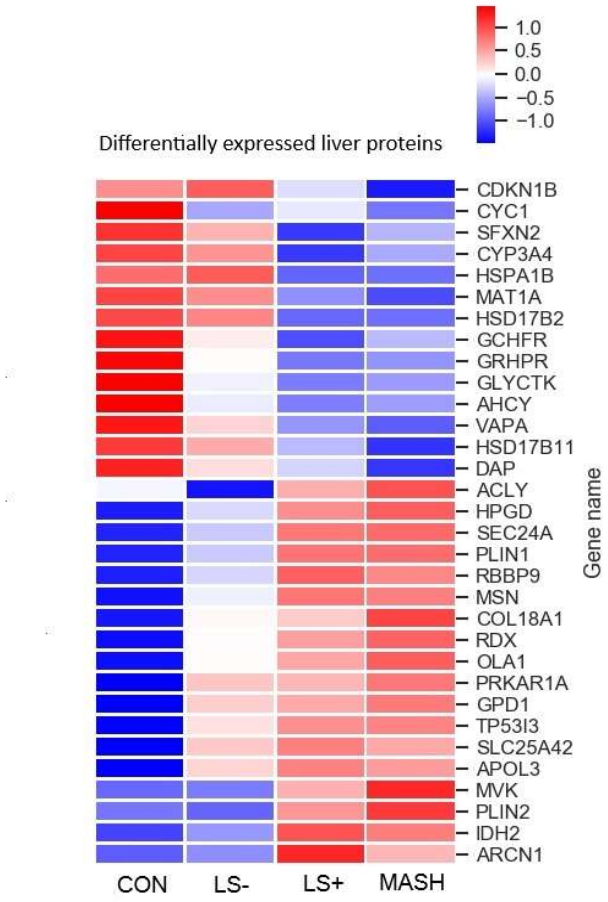

Figure 2. Heat map of differentially expressed liver proteins in CON, LS-, LS+ and MASH.

Table 2. Differentially expressed proteins in **liver tissue** in CON, LS-, LS+ and MASH identified by untargeted proteomics analyses. * q value (FDR adjusted value < 0.05) compared with CON. † q value (FDR adjusted value < 0.05) compared with LS-.

Protein name	Gene name	CON Log2 intensity	LS- Log2 intensity	LS+ Log2 intensity	MASH Log2 intensity	Location in cell	Tissue specificity	Main function(s)
Upregulated liver proteins in SWO/MASLD groups								
Metabolism								
Isocitrate dehydrogenase 2	**IDH2**	22.57	22.81	22.97*	23.03*	M,C,PX	Low	TCA
Glycerol-3-phosphate dehydrogenase 1	**GPD1**	22.12	22.71*	22.86*	22.84*	C	Low	CaM,LiM,LiB
OBG like ATPase 1	**OLA1**	18.86	19.20*	19.33*	19.35*	C	Low	CP, ATPH, GTPH
ATP citrate lyase	**ACLY**	18.40	18.06	18.76†	18.72†	C	Low	ACoA, LiM, LiB

 doi:10.20944/preprints202412.2367.v1

Mevalonate Kinase	**MVK**	17.99	18.11	18.79	18.92*†	C,PX	Low	ChoB, ChoM, LiM, LiB, SterB, SterM
15-hydroxyprostaglandin dehydrogenase	**HPGD**	18.07	18.77	19.37*†	19.32*	C, N	Placenta, liver, GI tract	FAM, LiM, PGM
Perilipin 1	**PLIN1**	14.24	14.99	16.09*†	16.25*†		Adipose tissue	LiMM, LiBi
Perilipin 2	**PLIN2**	15.09	15.08	16.87†	17.09†		Adipose tissue	LiMM, LiBi
Transport and carriers								
Apolipoprotein 3	**APOL3**	15.03	16.21*	16.51*	16.64*	C	Low	LiT
Solute carrier family 25 member 42	**SLC25A42**	15.03	16.31*	16.51*	16.57*	M	Liver	MTC, MTT, ADPT,ATPT, AMPT, ACoAT
Archain 1	**ARCN1**	18.23	18.26	18.38*†	18.31	V, ER	Low	ERGT, PT
Protein transport protein Sec24A	**SEC24A**	16.65	16.81	17.00*†	17.01*†	V	Low	ERGT, PT
Cytoskeleton, ECM and signal transduction								
Collagen type XVIII alpha 1 chain	**COL18A1**	18.62	19.11*	19.23*	19.40*	ECM	Liver	EMO
Radixin	**RDX**	20.70	20.93*	20.98*	21.04*	PM	Adrenal gland	CO, CA, ST
Moesin	**MSN**	20.38	20.96*	20.93*	20.76*	PM	Low	CO, CA, ST
Protein kinase cAMP-dependent type I regulatory subunit alpha	**PRKAR1A**	18.37	18.61*	18.64*	18.67*	C	Low	cAMP, ST
Cell, quality, cell cycle, and apoptosis								
Tumor protein p53 inducible protein 3	**TP53I3**	13.96	15.13*	15.84*	16.03*†	C	Intestine	Apop(+), SR
Retinoblastoma binding protein 9	**RBBP9**	18.01	18.17	18.31*	18.28*	N	Low	SH, TS, CCR
Downregulated liver proteins in SWO/MASLD groups								
Metabolism								

 doi:10.20944/preprints202412.2367.v1

Glycerate kinase	**GLYCKTK**	19.80	19.36*	19.09*	19.15*	C, G	Liver	FC, SD
Glyoxylate hydroxypyrovate dehydrogenase	**GRHPR**	24.04	23.82	23.59*†	23.69*	C, N	Liver	GlyoxM, PyroM
GTP cyclohydrolase I feedback regulator	**GCHFR**	20.09	19.70*	19.51*	19.55*	C, N	Liver	RP
Methionine adenosyltransferase 1A	**MAT1A**	21.67	21.57	21.38	21.34*†	C	Liver	1CM, MT, MetC
Adenosylhomocysteinase	**ACHY**	22.53	22.22*	22.08*	22.13*	C	Low	1CM, MT
Hydroxysteroid 17-beta dehydrogenase 2	**HSD17B2**	19.79	19.32	19.00*	18.94*	ER	Liver, intestine, placenta	LiB, LiM, SteB
Hydroxysteroid 17-beta dehydrogenase 11	**HSD17B11**	19.51	19.33	19.98	18.82*	ER, LD	Immune cells, intestine	LiB, LiM, SterB, AndC, EstB
Cytochrome P450 family 3 subfamily A member 4	**CYP3A4**	21.85	21.71	21.01*†	21.19	C, ER	Liver	FAM, CholM, LiM, LiB, SterB, SterM, DrugM
Mitochondrial								
Sideroflexin 2	**SFXN2**	17.88	17.36	17.14*†	17.65	M	low	MTTT, AAT
Cytochrome b-c1 complex (CIII)	**CYC1**	19.74	19.35*	19.35*	19.23*	M	low	ET, ATPS, RCP
Intracellular transport and carriers								
VAMP associated protein A	**VAPA**	19.30	19.25	19.14	19.06*†	ER, N, PM	Low	ERGT, PT, MF
Cell quality, cell cycle, apoptosis								
Death associated protein	**DAP**	17.97	17.65	17.44	17.24*†	V, M, N	Pancreas	Autop(-), Apop(-), NFkaBTF (-)
Heat shock protein family A (Hsp70) member 1B	**HSPA1B**	20.93	20.97	20.65†	20.78	V, C, N	Vagina	CHA, PF, SR

 doi:10.20944/preprints202412.2367.v1

Cyclin-dependent kinase inhibitor	**CDKN1B**	14.78	14.83	14.40	13.49†	N, V	Low	CCP

Location in cell: C, Cytosol; ECM, Extra cellular matrix; ER, Endoplasmatic reticulum; G, Golgi apparatus; LD, Lipid droplets; M, Mitochondria; N, Nucleus; PM, Plasma membrane; PX, Peroxisome; V, Vesicles

Main function: AAT, Amino acid transport (serine); ACoA, Acetyl CoA; ACoAT, Acetyl CoA transport; ADPT, ADP transport; ADPT, , AMP transport; AMPT; AndC, Androgen catabolism; Apop(+), Positive regulator of cell apoptosis; Apop(-), Negative regulator of cell apoptosis; ATPH, ATP hydrolysis; ATPS, ATP synthesis; ATPT, ATP transport; Autop(-), Negative regulator of autophagia; CA, Cell adhesion; CaM, Carbohydrate metabolism; cAMP, Cyclic adenosine monophosphate; CCR, Cell cycle regulator; CHA, Chaperone; ChoB, Cholesterol biosynthesis; ChoM, Cholesterol metabolism; CO, Cytoskeleton organization; CP, Cell proliferation; CCP, Cell cycle progression; DrugM, Drug metabolism; EMO, Extracellular matrix organization; ERGT, Endoplasmatic reticulum-Golgi apparatus transport; EstB, Estrogen biosynthesis; ET, Electron transport; FAM, Fatty acid metabolism; FC, Fructose catabolism; GlyoxM, Glyoxylate metabolism; GTPH, GTP hydrolysis; LiB. Lipid biosynthesis, LiBi, Lipid binding; LiM, Lipid metabolism; LiMM, Lipid metabolism modulator; LiT, Lipid transport; MetC, Methionine catabolism; MF, Membrane fusion; MT, Methylation; MTC, Mitochondrial carrier (ACoA transport into mitochondria in exchange for ATP/ADP/AMP); MTTT, Mitochondrial transmembrane transport; NFkaBTF(-), Negative regulator of NF-Kappa Beta transcription factor; PF, Protein folding; PGM, Prostaglandin metabolism (interleukins, eicosanoids etc) ; PT, protein transport; PyroM, Pyrovate metabolism; RCP, Respiratory chain protein; RP, Regulatory protein (phenalyalanine metabolism); SD, Serine degradation; SH, Serine hydrolase (unidentified substrates); SR, Stress response; ST, Signal transduction; SterB, Steroid biosynthesis; SterM, Steroid metabolism; TCA, Tricarboxylic acid cycle; Ts, Tumor suppressor; 1CM, One carbon metabolism

Six of the 14 downregulated proteins and three of the 18 upregulated proteins were 'liver specific' indicating an impaired synthesis of proteins in the liver (annotations were retrieved from the Human Protein Atlas [ref: https://pubmed.ncbi.nlm.nih.gov/21752111/]).

The DEPs grouped primarily in three predominant significance patterns: 1) Significant up-or downregulation in the MASLD groups (12 proteins) vs. CON with otherwise no significance among the four groups 2) Significant up- or downregulation between LS+ *or* MASH vs. CON and/or LS-. (ten proteins) 3) Significant up-or downregulation between LS+ *and* MASH combined vs. CON and/or LS- (seven proteins).

Six proteins were significantly altered in the MASH group compared with LS+, LS- and CON. One protein was upregulated (mevalonate kinase (**MVK**)) and five proteins were downregulated (hydroxysteroid 17-beta dehydrogenase 11 (**HSD17B11**), cyclin-dependent kinase inhibitor 1B (**CDKN1B**), death associated protein (**DAP**)**,** methionine adenosyltransferase 1A (**MAT1A**)) and VAMP associated protein A (**VAPA**). Four proteins were significantly altered in the LS+ group compared with remaining groups; One was up-regulated (archain 1 (**ARCN1**)) and three were downregulated (cytochrome P450 family 3 subfamily A member 4 (**CYP3AB**), sideroflexin-2 (**SFXN2**), and heat shock protein family A (Hsp70) member 1B (**HSPA1B**).

3.1.2. Differentially Expressed Upregulated Liver Proteins (Table 2 and Figure 2)

Amongst the 18 upregulated proteins, 12 proteins showed the highest intensities in the MASH group and six proteins showed the highest intensities in the LS+ group. None of the proteins expressed highest intensity in LS- group.

 doi:10.20944/preprints202412.2367.v1

When we sorted the upregulated proteins according to their main biological functions, the ”metabolism” group (proteins associated with primary cellular metabolic functions) comprised the highest number of proteins (eight proteins, **IDH2, GPD1, OLA1, MVK, HPGD, PLIN1, PLIN2**). As previously mentioned, **MVK** was the only upregulated DEP in MASH.

The perilipins (perilipin 1 (**PLIN1**) and perilipin 2 (**PLIN2**)) coat lipid droplets and are otherwise known to be highly expressed in adipocytes [21]. Out of the 32 hepatic DEPs **PLIN1** and **PLIN2** were the proteins with highest fold changes (around 3), but whereas **PLIN1** was 3-fold higher in LS+ and MASH compared to CON (q-value = 0.006) for **PLIN2** this 3-fold increase was observed between LS+/MASH and LS-, with no statistical significance when compared to CON.

Other liver proteins with significant up-regulation grouped in ‘intracellular transport proteins’ (four proteins) and proteins related to the cytoskeleton, intracellular signal transduction and extracellular matrix formation (five proteins). In the former group we found apolipoprotein 3 (**APOL3**), a lipid transporter which showed a 1-2.5-fold increase in the MASLD groups. Two proteins from the latter group, moesin (**MSN**) and radixin (**RDX**) were significantly upregulated in all three MASLD groups. Together with the protein ‘ezrin’, **MSN** and **RDX** are recognized as the ‘ezrin/radixin/Moesin (ERM) family’ [22]. Lastly, tumor protein p53 inducible protein 3 (**TP53I3**) was highly upregulated protein with tripled intensity in MASH and LS+ and doubled intensity in LS- when compared to CON.

3.1.3. Differentially Expressed Downregulated Liver Proteins (Table 2 and Figure 2)

Amongst the downregulated DEPs, 50% had the lowest intensities in MASH and 50% had the lowest intensities in LS+. None of the downregulated proteins had lowest intensities in LS-.

The largest groups of proteins (eight proteins; **GLYCKTK**, **GRHDR**, **GCHFR**, **MAT1A**, **ACHY**, **HSD17B2**, **HSD17B11**, **CYP3A4**) belonged to the ‘metabolism’ group. Glycerate kinase (**GLYCKTK**) which is involved in the catabolism of serine and metabolism of fructose was significantly downregulated in all three MASLD groups**.** Cytochrome P450 family 3 subfamily A member 4 (**CYP3A4**) was significantly downregulated in LS+.

3.1.4. Visceral Adipose Tissue

In VAT we found 59 DEPs between the four groups *(Table 3 and Figure 3)*. In VAT 42 proteins (71%) were upregulated and 17 proteins (29%) were significantly downregulated. Moreover, we observed considerable differences in protein intensities with up to 8.5-fold higher or lower intensities between groups (primarily CON vs. one or more of the MASLD groups) for specific proteins. Significant differences for a given DEP between the groups were predominantly observed between the MASLD groups collectively and CON (34 upregulated and nine downregulated) followed by significance between MASH/LS+ and LS-/CON (four upregulated and two downregulated) with the rest of the proteins (four upregulated and five downregulated) showing other significance patterns.

Table 3. Differentially expressed proteins in **visceral adipose tissue** identified by untargeted proteomics analysis in CON, LS-, LS+ and MASH. * q value (FDR adjusted value < 0.05) compared with CON. † q value (FDR adjusted value < 0.05) compared with LS-. § q value (FDR adjusted value < 0.05) compared with LS+.

Protein name	Gene name	CON Log2 intensity	LS- Log2 intensity	LS+ Log2 intensity	MASH Log2 intensity	Location in cell	Tissue specificity	Main function(s)
Upregulated VAT proteins in MASLD								
Metabolism								

 doi:10.20944/preprints202412.2367.v1

L-lactate dehydrogenase B chain	**LDHB**	16.53	17.96*	18.51*	18.40*	C	Heart, kidney	CM, PyrvM,Ferm
Inorganic pyrophosphatase	**PPA1**	13.47	15.30*	15.28*	15.68*	C	Low	PhosM
Lipid metabolism								
Sulfotransferase 1A1	**SULT1A1**	13.36	14.96*	14.50	15.36*	C	Liver	CateM, LiM, SterM, XM
Fatty aldehyde dehydrogenase	**ALDH3A2**	12.41	14.19*	14.09*	14.37*	PXM, ERM	Low	FAM, LiM, SB
Aldo-keto reductase family 1 member C1	**AKR1C1**	16.83	18.12*	18.28*	18.47*	C	Liver	PM, SterM
3-oxo-5-beta-steroid 4-dehydrogenase	**AKR1D1**	14.86	16.97*	17.16*	17.85*	C	Liver	AndM, BAB, ChoC, SterM
Aldo-keto reductase family 1 member B	**AKR1B1**	13.24	14.44	14.42*	14.45*	C	Adrenal gland	CM(PP), SteM, PGM, SIGM, SteM,
Aldo-keto reductase family 1 member C3	**AKR1C3**	15.07	16.06*	16.51*	16.53*	C	Liver	ProglM, AndM, CellD(+), Apop(+) ROSM(+)
Liver carboxylesterase 1	**CES1**	17.31	18.45*	18.95*	18.94*	ER	Liver	FAM, XM, ChoB
Epoxide hydrolase 1	**EPHX1**	15.91	17.91*	17.95*	17.78*	ER	Liver, adrenal gland	AHC, DtX
Alkylglycerone phosphate synthase	**AGPS**	7.80	10.68*	10.68*	10.16*	PX	Low	LiB, LiM
Mitochondrial								
Mitochondrial carnitine/acylcarnitine carrier protein	**SLC25A20**	11.57	13.17	13.02*	13.36*	M	Low	CarnS

 doi:10.20944/preprints202412.2367.v1

Sulfide:quinone oxidoreductase, mitochondrial	**SQOR**	13.72	12.83	12.89	13.85†§	M	Low	H_2SM
Inflammation								
Complement C1q subcomponent subunit C	**C1QC**	15.19	16.37*	16.61*	16.26*	XC (extra cellular)	Lymphoid tissue (monocytes)	ComP, ImR(+)
Complement C1r	**C1QR**	12.93	14.41*	14.10*	14.00*	XC	Lymphoid tissue (monocytes)	ComP, ImR(+)
Alpha-1-microglobulin	**AMBP**	14.86	16.41*	16.27*	16.59*	G,S,XC	Liver	HVI, ImR(-)
Intracellular transport and carriers								
Member RAS oncogene family	**RAB5C**	15.49	16.45*	16:36*	16.50*	EN	Low	PT
VPS35 endosomal protein sorting factor like	**VPS35**	14.76	15.43*	15.43*	15.69*	EN, PM	Low	GPMT, PT
Coatomer subunit beta’	**COPB2**	13.56	14.27*	14.41*	14.37*	C	Low	ERGT, PT
ADP-ribosylation factor 3	**ARF3**	15.05	16.11*	16.11*	16.13*	ER	Brain	ERGT, PT
MAL proteolipid protein 2	**MAL2**	11.19	14.12*	14.23*	14.42*	PM	Esophagus	TC (PIGR)
Cytoskeleton and ECM								
Keratin, type II cytoskeletal 1	**KRT1**	14.85	16.45*	16.06*	16.35*	PM	Skin	CO, ST, ComA
Vimentin	**VIM**	21.16	22.49*	22.47*	22.49*	PM,CS, N	Low	CO, HVI
Collagen alpha-2 (IV) chain	**COL4A2**	18.08	19.55*	19.90*	19.92*	ECM	Placenta	EMO
Tubulin beta-2A chain	**TUBB2A**	14.90	15.41	15.80*	15.87*	CS	Brain	CO, MCC
Lipoma-preferred partner	**LPP**							
Signal transduction and								

 doi:10.20944/preprints202412.2367.v1

regulation, apoptosis								
Tyrosine 3-monooxygenase	**YWHAZ**	18.42	19.21*	19.28*	19.44*	C, N	low	ST, Apop(-), Angio(+)
Phospholysine phosphohistidine inorganic pyrophosphate phosphatase	**LHPP**	12.19	13.88*	13.90*	13.71*	C	Brain	PDP
Annexin A5	**ANXA5**	17.59	18.94*	19.15*	19.13*	NM	Low	ST, BC(-), Apop(-)
Pleckstrin homology-like domain family B member 1	**PHLDB1**	12.23	13.88*	13.95*	13.86*	N, MiS	Brain	Reg
Dual specificity mitogen-activated protein kinase kinase 1	**MAP2K1**	11.92	13.10*	13.29*	13.49*	C, PM	Low	MAPKSC(+), PPARGSC(+)
Receptor-type tyrosine-protein phosphatase S	**PTPRS**	9.16	12.15*	11.74*	10.86	C, PM	Low	ST, MAPK(-), ImR(-)
Cell cycle, cell quality, and apoptosis								
Atlastin-3	**ATL3**	12.63	14.00*	14.24*	14.21*	ER	Low	ERQ
Reticulon-4	**RTN4**	13.33	13.90	14.17*	14.28*	ER	Low	ERS, Angio(+), Infl(+)
Crystallin alpha B	**CRYAB**	18.29	20.31*	20.76*	20.62*	C, PM	Muscle	CHA
Heat shock protein beta-6	**HSPB6**	16.24	18.22*	18.23*	18.35*	C, G	Muscle	CHA, SR, Angio(+)
Heterogeneous nuclear ribonucleoproteins A2/B1	**HNRNPA2B1**	16.40	17.68*	17.63*	17.69*	N	Low	mRNAp, mRNAs, mRNAt, HVI, ImR(+)
Parkinsonism associated deglycase	**PARK7**	15.51	17.17*	16.96*	17.11*	C, N	Low	CHA, PRep, PDeglyc, OxSS, MtHom

 doi:10.20944/preprints202412.2367.v1

Follistatin-related protein 1	**FSTL1**	10.56	11.50*	11.67*	11.98*	C, V	Low	CP, CD
Coactosin-like protein	**COTL1**	14.19	15.28*	15.32*	15.25*	C	Blood, lymphoid tissue	CHA, LeuS
Miscellaneous								
Myoglobin	**MB**	9.99	12.72*	12.05	13.07*	C	Muscle	OxT, OxR
Cystatin-B	**CSTB**	16.15	17.57*	17.47*	17.63*	C, N	Esophagus, tongue	Pro(-)
Unknown function								
FUN14 domain-containing protein 2	**FUNDC2**	12.99	14.22*	14.31*	14.23*	N, M	Low	MTautop
Downregulated VAT proteins in MASLD								
Mitochondrial metabolism								
2-oxoisovalerate dehydrogenase subunit alpha, mitochondrial	**BCKDHA**	13.00	12.43	11.32*	11.04*	M	Low	BCAAC
Pyruvate dehydrogenase protein X component, mitochondrial	**PDHX**	13.88	12.32*	12.31*	11.24*	M	Low	AcoAB, PyrvM
ATP synthase subunit alpha, mitochondrial	**ATP5A1**	18.58	17.85*	17.89*	17:54*	M	Low	ATPsyn
GTP:AMP phosphotransferase AK3, mitochondrial	**AK3**	16.21	15.25*	15.08*	15.51*	M	Low	NPI
Sulfide:quinone oxidoreductase, mitochondrial	**SQOR**	13.72	12.83	12.89	13.85†§	M	Low	H_2SM
Lipid metabolism								
Very-long-chain enoyl-CoA reductase	**TECR**	15.21	14.34*	14.37*	14.33*	ER	Low	FAB, FAE, FAM, LiB, LiM, SteM, SM

 doi:10.20944/preprints202412.2367.v1

Enoyl-CoA delta isomerase 1, mitochondrial	**ECI1**	15.00	14.49	14.13*	13.98*†	M	Muscle	FAOX, FAM, LiM
Cytochrome b5	**CYP5A**	17.46	16.51*	16.47*	16.00*	C, V	Liver	ET
Signal transduction								
Calcium/calmodulin dependent protein kinase II delta	**CAMK2**	14.66	14.04*	13.70*	13.92*	C,PM	Low	CaB, ST
Intracellular transport								
AP-1 complex subunit mu-1	**AP1M1**	15.54	13.93*	13.93*	14.36	C, G	Low	PT, HVI
Cytoskeleton, ECM and signaling								
Tight junction protein 2	**TJP2**	12.89	11.71*	11.22*	11.05*	PM, CJ	Low	CA,TJ
Cell cycle, cell quality, and apoptosis								
SH3 domain-containing kinase-binding protein 1	**SH3KBP1**	14.08	12.72*	12.65*	13.08	CS	Low	ST, CO, CA
Serine/threonine-protein phosphatase 2A activator	**PTPA**	13.94	13.01*	13.85†	13.01	C, N	Low	PF, DNArep, CCP
Antioxidant defense								
Probable hydrolase PNKD	**PNKD**	13.28	12.41*	12.26*	12.22*	C, M	Low	GlutB(+)
Miscellaneous								
Sperm associated antigen-17	**SPAG17**	20.56	18.68*	18.70*	18.88*	C, CS	Testis, epididymis, brain	CilB, CiF
Family with sequence similarity member A2	**FAM114A2**	11.54	10.26*	11.30†	11.09	V	low	PuNB
Hemoglobin subunit alpha	**HBA1**	25.86	24.55*	24.36*	25.02	C	Bone marrow	OxT

 doi:10.20944/preprints202412.2367.v1

Location in cell: C, Cytosol; CJ, Cell junction; CS, Cytoskeleton; ECM, Extra cellular matrix; EN, Endosome; ER, Endoplasmatic reticulum, ERM, Endoplasmatic reticulum membrane; G, Golgi apparatus; M, Mitochondria; MiS, Mitochondrial spindle; N, Nucleus, NM, Nuclear mem; PM, Plasma membrane; PX, Peroxisome; PXM, Peroxisome membrane; S, Secreted; V, Vesicle; XC, Extra cellular

Main function: ACoAB, Acetyl CoA biosynthesis; AHC, Aromatic hydrocarbon catabolism; AndM, Androgen metabolism; Angio(+), Postitive regulator of angiogenesis; Apop(+), Positive regulator of cell apoptosis; Apop(-), Negative regulator of cell apoptosis; ATPsyn, ATP synthesis; BAB, Bile acid biosynthesis; BC(-), Negative regulator of blood coagulation (anti-coagulant); BCAAC, Branched chain amino acid; CA, Cell adhesion; CaB, Calcium binding; CarnS, Carnitine shuttle; CateM, Cathecolamin metabolism; CCP, Cell cycle progression; CD, Cell differentiation; CellD(+), Positive regulator of cell death; CHA, Chaperone; ChoB, Cholesterol biosynthesis; ChoC, Cholesterol catabolism; CilB, Cillium biosynthesis; CilF, Cillium function; CM, Carbohydrate metabolism; CM(PP), Carbohydrate metabolism (polyol pathway); CO, Cytoskeleton organization; ComA, Complement activation; ComP, Complement pathway; CP, Cell proliferation; DNArep, DNA repair; Dtx, Detoxification; EMO, Extra cellular matrix, ERGT, Endoplasmatic reticulum-Golgi apparatus transport; ERS, Endoplasmatic reticulum stabilization; ERQ, Endoplasmatic reticulum quality; ET, Electron transport; FAB, Fatty acid biosynthesis; FAE, Fatty acid elongation; FAM, Fatty acid metabolism; FAOX, Fatty acid beta oxidation; Ferm, Fermentation; GlutB(+), Positive regulator of gluthation biosynthesis; GPMT, Golgi-plasma membrane transport; HVI, Host-virus interaction; H2SM, Hydrogene sulfide metabolism; ImR(+), Positive regulator of immune response; ImR(-), Negative regulator of immune response; Infl(+), Inflammation; LeuS, Leukotriene synthesis; LiB, Lipid biosynthesis; LiM, Lipid metabolism; MAPK(-), Negative regulator of MAP kinase; MAPKSC(+), Positive regulator of MAPK signaling cascade; MMC, Miotic cell cycle; mRNAp, mRNA processing; mRNAs, mRNA splicing; mRNAt, mRNA transport; MTautop, Mitochondrial autophagia; MtHom, Mitochondrial homeostasis; NPI, Nucleoside phosphate interconversion; OxR, Oxygen transport; OxSS, Oxygen stress sensor; OxT, oxygen transport; PDeglyc, Proetin deglucase activity; PDP, PF, Protein folding; Protein dephosphorylation; PGM, Prostaglandin metabolism; PhosM, Phosphate metabolism; PM, Progesterone metabolism; PPARGSC(+), Positive regulator of PPRAG signaling cascade; PRep, Protein repair; Pro(-), Protease inhibitor; PT, Protein transport; PuNB; Purine nucleotide binding; PyrvM, Pyruvate metabolism; Reg, Regulator; ROSM(+), Positive regulator of reactive oxygen species; SIG, Signalling; SB, Sphingolipid biosynthesis; SM, Sphingolipid metabolism; SR, Stress response; ST, Signal transduction; SterM, Steroid metabolism; TJ, Tight junction; TC;, Transcytosis; XM, Xenobiotic metabolism

 doi:10.20944/preprints202412.2367.v1

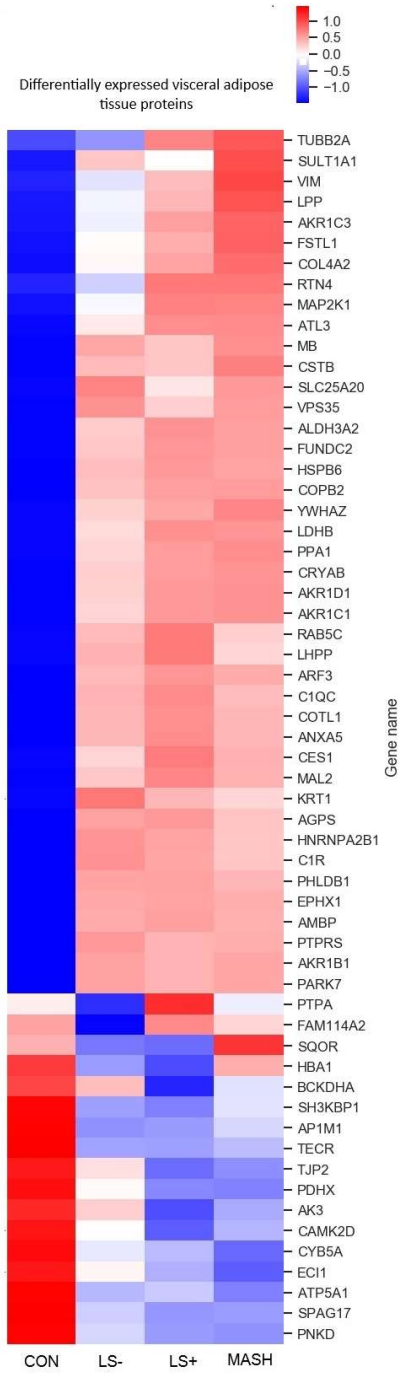

Figure 3. Heat map of differentially expressed visceral adipose tissue proteins in CON, LS-, LS+ and MASH.

Only a single protein, the mitochondrial sulfide:quinone oxidoreductase (**SQOR**), was exclusively downregulated in MASH. LS+ had significant upregulation of the serine/threonine-protein phosphatase 2A activator (**PTBA**), a chaperone protein governing DNA repair and protein folding.

 doi:10.20944/preprints202412.2367.v1

3.1.5. Differentially Expressed Upregulated VAT Proteins (Table 3 and Figure 3)

Upregulated proteins were grouped according to main function and are depicted in Table 3. Nine of the upregulated proteins were involved in lipid metabolism. Notably, four of these (hydroxysteroid dehydrogenase (**AKR1C1**), steroid 5β-reductase (**AKR1D1**), aldose reductase **AKR1B1,** hydroxysteroid dehydrogenase (**AKR1C3**)) belonged to the aldo-keto reductase family.

We found upregulation of the complement system through complement C1 subcomponents **C1r** and **C1q**. They assemble with subcomponent C1s to form the C1 complex which is the first component in the serum complement system and activator of the classical (antigen-antibody) component pathway.

Other proteins with significant upregulation belonged to intracellular signaling, cytoskeletal and extracellular matrix proteins and proteins related to cell/organelle quality including several chaperones (heat shock protein beta-6 (**HSPB6**), crystallin alpha B (**CRYAB**), parkinsonism associated deglycase (**PARK7**) and coactosin-like protein (**COTL1**). Of these, **HSPB6** also functions as a stress sensor [23]

Notably, myoglobin (**MB**), a protein found primarily in muscle with excellent oxygen binding and reservoir capacities showed prominent upregulation with 4-6 times higher expression in MASLD groups than CON. Lastly, several proteins aiding angiogenesis (e.g., tyrosin-3 monooxygenase (**YWHAZ**), **RTN4 and HSPB6**) were upregulated in MASLD groups.

3.1.6. Differentially Expressed Downregulated VAT Proteins (Table 3 and Figure 3)

The 17 downregulated proteins were scattered over several groups.

Five proteins were mitochondrial proteins and included the ATP synthase subunit alpha (**ATP5A1**), which is one of the core components of the ATP synthase complex in the electron transport chain.

In addition, the mitochondrial 2-oxoisovalerate dehydrogenase subunit alpha (**BCKHDA**) was also significantly downregulated in LS+ and in MASH by 2-fold compared with CON. **BCKHDA** is the alpha subunit of the decarboxylase component of the branched chain dehydrogenase (BCKD) complex that catalyzes the second and irreversible step in the catabolism of branched chain amino acids valine, leucine and isoleucine.

3.1.7. Associations Between VAT and Liver Tissue in MASLD: Correlation Data (Table 4).

24 proteins correlated significantly between VAT and liver tissue (*Table 4*). Of these, 22 correlated positively and two correlated negatively. The protein with the highest correlation coefficient was Hemoglobin subunit gamma-1 (**HBG1**) which is the gamma chain of fetal hemoglobin ($\alpha 2\gamma 2$) (pearson $r = 0.71$). Interestingly, angiotensinogen (**AGT**), the precursor of angiotensin was the protein with the second strongest correlation coefficient.

Table 4. The 24 significant FDR adjusted proteins by correlation analysis between VAT and liver tissue.

Protein name	Gene name	q-value	Pearsons *r*	Location in cell	Tissue specificity	Main function(s)
Hemoglobin subunit gamma-1	**HBG1**	0.0000	0.717	C	Placenta	FetalHG, Oxb, OxT
Immunoglobulin heavy constant alpha 2	**IGHA2**	0.0000	0.630	PM, Secreted	Low	ImR
Angiotensinogen	**AGT**	0.0000	0.624	Secreted	Liver	RAAS, BPReg
Ribosyldihydronicotinamide dehydrogenase [quinone]	**NQO2**	0.0000	0.603	C	Low	DeTox, OxStress protector
Glutathione S-transferase theta-1	**GSTT1**	0.0001	0.595	C	Breast	GluthB, GluthM

 doi:10.20944/preprints202412.2367.v1

NAD(P)HX epimerase	**NAXE**	0.0001	0.586	C, N	Low	NAD(P)HXrep
Immunoglobulin heavy constant mu	**IGHM**	0.0002	0.557	PM, Secreted	Low	ImR
Complement C4-A	**C4A**	0.0005	0.554	Secreted	Liver	CP, ImR(+)
Copine-1	**CPNE1**	0.0006	0.535	N, NM	Low	TNFaSig, TF
Enoyl-CoA hydratase domain-containing protein 3, mitochondrial	**ECHDC3**	0.0006	0.532	M	Liver, muscle	FAM, LiM
Complement C4-B	**C4B**	0.0010	0.521	Secreted	Liver	CP, ImR(+)
Afamin	**AFM**	0.0025	0.5	ECM, Se	Liver	PT, FAB
N-acetylneuraminate lyase	**NPL**	0.0452	0.492	VE, PM	Blood	CM
Epsin-1	**EPN1**	0.0041	0.491	PM, C	Low	Endocytosis
Acyl-coenzyme A thioesterase 1	**ACOT1**	0.0064	0.476	M	Liver	FAM, AcoAM
Phosphoglucomutase-1	**PGM1**	0.0068	0.473	C	Muscle	CM, GluM
Glycogenin-2	**GYG2**	0.0290	0.44	C, N	Adipose tissue, brain, breast	GlycB
Tyrosine-protein kinase CSK	**CSK**	0.0313	0.433	C, V	Lymphoid tissue	Reg, Imm
Heat shock protein HSP 90-alpha	**HSP90AA1**	0.0360	0.428	C	Vagina	Cha, HVI, SR
Interferon-induced protein with tetratricopeptide repeats 1	**IFIT1**	0.0367	0.426	C	Low	HVI, Imm
Histidine-rich glycoprotein	**HRG**	0.0455	0.415	Secreted	Liver	Angio(+), BC, Chem
Tetratricopeptide repeat protein 38	**TTC38**	0.0498	0.411	C, secreted	Liver, intestine	Unknown
60S ribosomal protein L38	**RPL38**	0.0453	-0.416	ER, C	Low	RibP, Translation
RAB14 member RAS oncogene family	**RAB14**	0.0450	-0.419	Er, C	Low	RibP, Translation

Oxb; oxygen binding, OxT; Oxygen transport, ImR; Immune response, RAAS; Renin-angiotensiogen-aldosterone-system, BPReg; Blood pressure regulator, DeTox; Detoxification process, OxStress; Oxidative stress, GluthB; Gluthation biosynthesis, GluthM; Gluthation metabolism, NAD(P)HXrep; Repairs NAD(P)H hydrates (NAD(P)HX), CP; Complement pathway, ImR; Immuneresponse, TNFaSig; TNF-alpha signalling,TF; transcription factor, FAM; Fatty acid metabolism, LiM; Lipid metabolism, PT; Protein transport, FAB; Fatty acid binding,AcoAM; Acetyl CoA metabolism, CM; Carbohydrate metabolism, GlycB; Glycogen breakdown, Imm; Adaptive immunity, Cha; Chaperone, HVI; Host-virus interaction Angio+; positive regulator of angiogenesis, BC; Blood coagulation, Chem; Chemotaxis, RibP; Ribosomal protein

Four of the ten proteins with highest correlation coefficients were related to the immune system; two were immunoglobulins (immunoglobulin heavy constant alpha 2 (**IGHA2**) and immunoglobulin heavy constant mu (**IGHM**)) and two belonged to the complement cascade, namely complement C4-A (**C4A**) and complement C4-B (**C4B**). The latter two are the components of the complement component C4, a central component of the classically activated pathway in the complement cascade.

Ribosyldihydronicotinamide dehydrogenase [quinone] (**NQO2**), glutathione S-transferase theta-1 (**GSTT1**) and NAD(P)HX epimerase (**NAXE**), proteins with the third, fourth fifth highest correlation coefficients are all involved in oxidative defense, detoxification and/or repair mechanisms.

 doi:10.20944/preprints202412.2367.v1

4. Discussion

No Overlapping DEPs Between VAT and Liver Tissue in Subjects with Obesity, MASLD and MASH

This paper describes the largest human study with evaluation of the associations between the proteome in VAT and liver tissue to date.

Understanding the metabolic and functional disturbances in VAT and liver tissue is central to the understanding of the underlying pathophysiology of MASLD as it may also provide information on the metabolic disease risk in general. Considerable clinical overlap exists between the MASLD conditions (liver steatosis vs. MASH) but possibly with distinct patterns for different disease states. Protein patterns could here serve as phenotype identifiers and guide us towards biomarker discovery in MASLD. In that context it is important to map the proteomic signatures in VAT in relation to MASLD, as future biomarkers could reflect VAT dysfunction and in addition may be able to predict the progression to MASH, liver fibrosis and liver cirrhosis.

Where the untargeted proteomics approach in tissue has previously been applied in human studies of other metabolic diseases, T2DM especially [24,25] MASLD remains relatively unexplored and there are no human studies for specific comparison for VAT and liver tissue proteomics in the context of severity of MASLD.

We hypothesized that we would find specific proteins that were simultaneously and significantly up-or downregulated in the two tissues but we found no such proteins.

Parallel to the lack of overlapping proteins, we also did not find evidence of the presence of a VAT specific proteome that reflected the degree of MASLD severity and in general we found very little difference in the protein expression patterns between the MASLD groups. For example, we did not find inflammatory proteins in VAT to be generally more upregulated in MASH patients. In fact, we found merely a single VAT protein which was significantly upregulated in MASH only, namely **SQOR. SQQR** catalyzes the primary step in the metabolism of hydrogen sulfide (H_2S) within the mitochondria[26]. H_2S is a gasotransmitter, which is toxic in high concentrations and at low concentrations acts cytoprotective and is involved in many different biological functions including anti-inflammatory and proinflammatory abilities[27]. However, from this data we are not able to conclude, whether **SQOR** is upregulated due to high H_2S amount in MASH.

Based on the protein expression patterns we generally observed the tendency of CON and LS- group together and LS+ and MASH group together or that the significance of a given protein (e.g., **AKR1B1, SLC25A20, RTN4, BCKDHA and ECI1**) was found between LS+ *and* MASH vs. CON but not LS- vs. CON. Yet, the log2 intensities for the given protein were often still numerically much higher or lower in LS- compared with CON and thus may indicate a distinct biological difference – probably obesity - between these groups despite the absence of histological liver steatosis in both groups. The observed expression patterns in VAT therefore appear to reflect the metabolic deterioration that is associated with central obesity. The severity of MASLD is linked to the degree of metabolic dysregulation[28]. Our analyses are unable to determine if the observed differences reflect common risk factors or if there is a direct link between metabolic dysfunction in VAT and MASLD severity. Of note, among the included participants, those with MASH and LS+ were more likely to have T2DM, they had a higher HOMA-IR, and had higher levels of plasma liver enzymes. This was, however, not clearly reflected in the VAT DEPs.

Changes in the VAT Proteome in Obesity, T2DM and MASLD

No previous studies have investigated the proteome profile in human VAT in relation to MASLD but several have explored the human obese VAT proteome in relation to T2DM [29–31], in metabolically healthy vs. unhealthy subjects with obesity [32] as well as differences between SAT and VAT from individuals with obesity [33]. Several of the other VAT upregulated DEPs found in our study have been identified in other human obesity/T2DM studies e.g., annexin (**ANXA5**)[29,37] , liver carboxyl esterase 1 (**CES1**)[37] (48), **C1QC** [37](48) and myoglobin (**MB)**[38] . Moesin (**MSN**), which we found upregulated in the liver has similarly been found upregulated in VAT and SAT in subjects

 doi:10.20944/preprints202412.2367.v1

with obesity[29] . In addition, we found upregulation of **C1QC**, which is the c-chain of the C1qof human complement subcomponent C1q was significantly upregulated in all three MASLD groups. Additionally, we found upregulation of the perilipins **PLIN1** and **PLIN2** in liver tissue but not VAT. **PLIN1** is believed to function as a lipid droplet protector that modulates the action of the hormone sensitive lipase in adipose tissue and thus helps regulate lipid metabolism. In its absence leanness is promoted on the expense of insulin resistance in PLIN1 knock-out mice[34]. **PLIN1** and especially **PLIN2** have previously been associated with the development of MASLD in rodent models and humans [35,36]**.**

We also note the relative 'overrepresentation' of downregulated DEPs related to mitochondrial function and metabolism – e.g., **BCKDHA, ATP5A1, PDHX, AK3 and SQOR,** the latter being the single VAT DEP significant in MASH only. Prominent downregulation of mitochondrial proteins and proteins related to the respiratory machinery in obesity has recently been recognized in a diet-induced obesity mouse model [39], but systematic human data are lacking. The significant downregulation of **BCKDHA** is interesting as plasma levels of branched chain amino acids (leucine, isoleucine and valine) have been reported to be increased in insulin resistant individuals with obesity. In addition, adipose tissue is recognized as an important site for BCAA catabolism[40] . Other studies have also reported significant downregulation in obese adipose tissue of the enzymes responsible for BCAA catabolism [41], including the branched chain ketoacid dehydrogenase complex (BCKDHC) of which the **BCKDHA** is a subunit and that catalyzes the irreversible catabolic step in BCAA breakdown.

Correlation Analyses Pinpoint Inflammatory and Detoxification Proteins

In the correlation analyses between VAT and liver, the top 10 positive correlations were dominated by inflammatory proteins and proteins involved in oxidative defense mechanisms and detoxification processes. This could point towards simultaneously upregulation and overlapping pathophysiology in the two tissues. It could be argued that the high abundance of secretory proteins (Table 4) amongst the proteins with high correlation scores represent 'contamination' of plasma and blood vessels in the two tissues. However, we would then have expected to see high correlation scores of other plasma proteins with very high abundance in plasma -e.g., albumin or hemoglobin subunit A (normal hemoglobin). But this was not the case. Rather, the finding of **IGHA2, IGHM, C4A and C4B** is probably reflective of synergy in intrahepatic and intra-adipose tissue antibody production as a systemic response to regulation of immune homeostasis and inflammation.

The protein with the highest correlation score was fetal hemoglobin gamma chain (**HBG1**). Under normal physiological conditions (except pregnancy) fetal hemoglobin only exists in very limited amounts in adults comprising <0.6 % of total hemoglobin[43]. The synthesis of fetal hemoglobin, which has higher oxygen affinity than hemoglobin is confined to a population of erythrocytes termed the F-cells[43].. The presence of **HBG1** and the high correlation score of 0.717 between the two tissues can only be speculative as there is very limited data on adult fetal hemoglobin in conditions other than β-thalassemia and sickle cell anemia. Also, we have not investigated the specific intensities of **HBG1** between MASLD groups and CON in VAT and liver. We can only speculate as to whether severe obesity and/or metabolic disease perhaps induce an increase in F-cell erythrocytes that are capable of producing hemoglobin gamma-chains? Further research into this finding is warranted.

Changes in the Liver Proteome in Relation to Obesity and MASLD

In the liver tissue we found a couple of DEPs that were upregulated or downregulated in MASH and LS+ exclusively, but it is difficult to conclude on any specific patterns, as the DEPs were very heterogenous both in function and cellular compartment. However, we did observe a tendency of the upregulated proteins to be related to lipid and cholesterol metabolism (**OLA1, ACLY, MVK, HPGD, APOL3, PLIN1 and PLIN2**) and to cytoskeleton and ECM reorganization (**COL18A1, RDX and MSN**). Upregulation of ECM proteins in MASLD have been recognized in a study by Yuan and

 doi:10.20944/preprints202412.2367.v1

colleagues, who analyzed the liver tissue proteome from 12 patients with obesity classified as metabolically healthy but with obesity and 44 patients with obesity and MASLD according to liver histology[44] (53). By gene ontology analysis, they furthermore report significant downregulation of mitochondrial oxidative phosphorylation through downregulation of components of the complex I (NADH dehydrogenase complex) and complex IV (cytochrome c oxidase) in MASLD subjects. In comparison, we found significant downregulation of complex III (**CYC1**) but this downregulation was equal in all MASLD groups compared with CON.

We have previously investigated the plasma proteome in a study cohort comprising of 48 individuals with and without MASLD and liver cirrhosis and validated a promising panel of plasma proteins in a mouse model[18] (18). Among the promising proteins we found the polymeric immunoglobin receptor **PIGR** to be significantly upregulated in MASLD and to increase with increase in liver disease (obese without MASLD, T2DM with MASLD and patients with cirrhosis). **PIGR** is a transmembrane glycoprotein, a Fc receptor, that enables transcytosis of immunoglobulins from the basolateral to the apical surface of epithelial cells, thus mediating the secretion of IgA and IgM[45]. We did not confirm the findings of upregulated PIGR in the present data in neither liver nor adipose tissue. However, we did discover MAL proteolipid protein 2 (**MAL2**) to be roughly 8-fold increased in all three MASLD groups compared with CON. **MAL2** was the protein showing the biggest difference in intensities between groups. This is interesting because **MAL2** is an essential component of the transcytotic machinery[46,47]and has previously been implicated in PIGR mediated transcytosis where depletion of **MAL2** blocked polymeric immunoglobulin receptor transcytosis in liver cells (the hep g2 cell line)[46] (55). Though data derived from cell lines should be evaluated with some caution the potential association between **MAL2** in VAT and PIGR found in plasma in two different MASLD cohort could is still noteworthy. Adding to this notion, the proteins with the second and the sixth strongest correlations between VAT and liver tissue were the heavy chains of precisely IgA and IgM (**IGHA2** and **IGHM**, respectively).

Strengths and Limitations

We wanted to explore potential overlapping DEPs in MASH between VAT and liver and to characterize the VAT proteome in MASH. The rationale was to assess common pathophysiological traits in the two tissues. However, this exploratory approach has limitations, that may hinder the true answer(s) to the hypotheses. By dividing the study cohort up into three MASLD groups based on histology and applying one-way ANOVA, we may have missed interesting and significant proteins. There are also some inherent drawbacks in proteomics studies in general. For instance, the generated data depend on the subjective threshold set for DEPs. In addition, the analysis discards most of the proteins and as a result focus on the significant DEPs which comprise only <0.1 % of the analyzed total proteome in the tissue. Furthermore, by filtering for 70% (meaning, that only proteins which are detectable in 70% of the samples enter the analysis) there is an inherent risk of filtering out proteins which were indeed significant in one group only. We may therefore have missed important proteins in one or more of the groups.Finally, the grouping of the study subjects according to the histopathological MASLD severity may pinpoint the weaknesses of the NAFLD activity score, as we observe very little difference in protein expression between the MASLD groups, particular between LS+ and MASH.

Proteomics studies and the generated data herein are in general difficult to compare due to significant heterogeneity in endpoints, grouping, analytical methodology (e.g., targeted vs untargeted approach) and data acquisition (use of FDR, considerations regarding significance). In addition, most studies have very low n, down to 4 per group[31], but typically n is around 10 per group. In comparison, our cohort consisted of 79 study subjects and the applied LC-MS analyses performed are of very high quality and robustness.

5. Conclusions

 doi:10.20944/preprints202412.2367.v1

Altogether we found no overlap of proteins in VAT and liver tissue and neither in VAT nor in liver tissue did we find a MASH specific protein pattern, as DEPs, especially in VAT tended to group according to obesity and not in relation to MASLD severity. Consequently, from this exploratory study and the data analyses here applied the contribution from VAT in MASLD pathophysiology is ambiguous. However, several immunomodulating proteins correlated significantly between liver and VAT and could address shared pathophysiological characteristics but whether immunomodulation in the VAT affects the immunomodulation in the liver cannot be concluded from the present study.

As this dataset comprises the largest human proteome dataset to date in study subjects with severe obesity and MASLD this data can be used to generate and support hypotheses in MASLD pathophysiology and further explore disease traits.

Author Contributions: Conceptualization, Julie Pedersen and Nicolai Jacob Albrechtsen; Formal analysis, Julie Pedersen and Lili Niu; Funding acquisition, Torben Hansen and Flemming Bendtsen; Investigation, Julie Pedersen, Viggo Kristiansen, Inge Marie Poulsen and Reza Serizawa; Methodology, Julie Pedersen, Lili Niu, Viggo Kristiansen, Reza Serizawa, Lise Lotte Gluud and Flemming Bendtsen; Project administration, Julie Pedersen, Torben Hansen and Flemming Bendtsen; Resources, Lise Lotte Gluud and Flemming Bendtsen; Software, Lili Niu and Nicolai Jacob Albrechtsen; Supervision, Torben Hansen, Lise Lotte Gluud, Sten Madsbad and Flemming Bendtsen; Validation, Lili Niu and Nicolai Jacob Albrechtsen; Visualization, Lili Niu; Writing – original draft, Julie Pedersen; Writing – review & editing, Julie Pedersen, Lili Niu, Nicolai Jacob Albrechtsen, Viggo Kristiansen, Inge Marie Poulsen, Reza Serizawa, Torben Hansen, Lise Lotte Gluud, Sten Madsbad and Flemming Bendtsen.

Funding: This research was funded by a Challenge Grant "MicroBLiver" (grant number NNF15OC0016692) from the Novo Nordisk Foundation.

Institutional Review Board Statement: In this section, you should add the Institutional Review Board Statement and approval number, if relevant to your study.

The study was conducted in accordance with the Declaration of Helsinki, and approved by the Institutional Review Board (or Ethics Committee) of NAME OF INSTITUTE (protocol code XXX and date of approval)." for studies involving humans. OR "The animal study protocol was approved by the Institutional Review Board (or Ethics Committee) of NAME OF INSTITUTE (protocol code XXX and date of approval)." for studies involving animals. OR "Ethical review and approval were waived for this study due to REASON (please provide a detailed justification)." OR "Not applicable" for studies not involving humans or animals.

Informed Consent Statement: The study protocols were approved by the Regional Scientific Ethics Committee (H-16030784 and H-16030782) in the Capital Region of Denmark and the Danish Data Protection Agency. The study was conducted in accordance with the Declaration of Helsinki. Oral and written informed consent were obtained from all study participants.

Data Availability Statement: The data presented in this study are available on request from the corresponding author. The data are not publicly available due to restrictions set by the Danish Data Protection Agency.

Acknowledgments: We would like to thank the MicroBLiver Research Consortium and project nurse Karen Lisa Hilsted.

Conflicts of Interest: The authors declare no conflicts of interest.

References

1. Rosen, E. D. & Spiegelman, B. M. What We Talk About When We Talk About Fat. *Cell* **156**, 20–44 (2014).
2. Ohlson, L.-O. et al. The Influence of Body Fat Distribution on the Incidence of Diabetes Mellitus: 13.5 Years of Follow-up of the Participants in the Study of Men Born in 1913. *Diabetes* **34**, 1055–1058 (1985).
3. Nielsen, S., Guo, Z., Johnson, C. M., Hensrud, D. D. & Jensen, M. D. Splanchnic lipolysis in human obesity. *J. Clin. Invest.* **113**, 1582–1588 (2004).
4. Tilg, H. & Moschen, A. R. Adipocytokines: mediators linking adipose tissue, inflammation and immunity. *Nat. Rev. Immunol.* **6**, 772–783 (2006).
5. Fontana, L., Eagon, J. C., Trujillo, M. E., Scherer, P. E. & Klein, S. Visceral Fat Adipokine Secretion Is Associated With Systemic Inflammation in Obese Humans. *Diabetes* **56**, 1010–1013 (2007).

6. Eckel, R. H., Grundy, S. M. & Zimmet, P. Z. The metabolic syndrome. *Lancet Lond. Engl.* **365**, 1415–1428 (2005).
7. Vanni, E. et al. From the metabolic syndrome to NAFLD or vice versa? *Dig. Liver Dis.* **42**, 320–330 (2010).
8. Yki-Järvinen, H. Non-alcoholic fatty liver disease as a cause and a consequence of metabolic syndrome. *Lancet Diabetes Endocrinol.* **2**, 901–910 (2014).
9. Hotamisligil, G. S., Shargill, N. S. & Spiegelman, B. M. Adipose expression of tumor necrosis factor-alpha: direct role in obesity-linked insulin resistance. *Science* **259**, 87–91 (1993).
10. Sun, K., Kusminski, C. M. & Scherer, P. E. Adipose tissue remodeling and obesity. *J. Clin. Invest.* **121**, 2094–2101 (2011).
11. Goossens, G. H. The role of adipose tissue dysfunction in the pathogenesis of obesity-related insulin resistance. *Physiol. Behav.* **94**, 206–218 (2008).
12. Xu, H. et al. Chronic inflammation in fat plays a crucial role in the development of obesity-related insulin resistance. *J. Clin. Invest.* **112**, 1821–1830 (2003).
13. Weisberg, S. P. et al. Obesity is associated with macrophage accumulation in adipose tissue. *J. Clin. Invest.* **112**, 1796–1808 (2003).
14. Younossi, Z. M. et al. The economic and clinical burden of nonalcoholic fatty liver disease in the United States and Europe. *Hepatology* **64**, 1577–1586 (2016).
15. Item, F. & Konrad, D. Visceral fat and metabolic inflammation: the portal theory revisited: Visceral fat and metabolic inflammation. *Obes. Rev.* **13**, 30–39 (2012).
16. Kakehashi, A. et al. Proteome Characteristics of Non-Alcoholic Steatohepatitis Liver Tissue and Associated Hepatocellular Carcinomas. *Int. J. Mol. Sci.* **18**, (2017).
17. Younossi, Z. M. et al. An exploratory study examining how nano-liquid chromatography–mass spectrometry and phosphoproteomics can differentiate patients with advanced fibrosis and higher percentage collagen in non-alcoholic fatty liver disease. *BMC Med.* **16**, (2018).
18. Niu, L. et al. Plasma proteome profiling discovers novel proteins associated with non-alcoholic fatty liver disease. *Mol. Syst. Biol.* **15**, e8793 (2019).
19. Wichmann, C. et al. MaxQuant.Live Enables Global Targeting of More Than 25,000 Peptides. *Mol. Cell. Proteomics MCP* **18**, 982–994 (2019).
20. Grinfeld, D., Aizikov, K., Kreutzmann, A., Damoc, E. & Makarov, A. Phase-Constrained Spectrum Deconvolution for Fourier Transform Mass Spectrometry. *Anal. Chem.* **89**, 1202–1211 (2017).
21. Greenberg, A. S. et al. Perilipin, a major hormonally regulated adipocyte-specific phosphoprotein associated with the periphery of lipid storage droplets. *J. Biol. Chem.* **266**, 11341–11346 (1991).
22. Karvar, S. et al. Moesin, an Ezrin/Radixin/Moesin Family Member, Regulates Hepatic Fibrosis. *Hepatol. Baltim. Md* (2019) doi:10.1002/hep.31078.
23. Li, F., Xiao, H., Zhou, F., Hu, Z. & Yang, B. Study of HSPB6: Insights into the Properties of the Multifunctional Protective Agent. *Cell. Physiol. Biochem.* **44**, 314–332 (2017).
24. Arderiu, G. et al. Type 2 Diabetes in Obesity: A Systems Biology Study on Serum and Adipose Tissue Proteomic Profiles. *Int. J. Mol. Sci.* **24**, 827 (2023).
25. Chen, Z.-Z. et al. Protein Markers of Diabetes Discovered in an African American Cohort. *Diabetes* **72**, 532–543 (2023).
26. Jackson, M. R., Melideo, S. L. & Jorns, M. S. Human sulfide:quinone oxidoreductase catalyzes the first step in hydrogen sulfide metabolism and produces a sulfane sulfur metabolite. *Biochemistry* **51**, 6804–6815 (2012).
27. Paul, B. D. & Snyder, S. H. H2S: a novel gasotransmitter that signals by sulfhydration. *Trends Biochem. Sci.* **40**, 687 (2015).
28. Younossi, Z. M. et al. Global epidemiology of nonalcoholic fatty liver disease—Meta-analytic assessment of prevalence, incidence, and outcomes. *Hepatology* **64**, 73–84 (2016).
29. Fang, L. et al. Analysis of the Human Proteome in Subcutaneous and Visceral Fat Depots in Diabetic and Non-diabetic Patients with Morbid Obesity. *J. Proteomics Bioinform.* **8**, 133–141 (2015).
30. Kim, S.-J. et al. A Protein Profile of Visceral Adipose Tissues Linked to Early Pathogenesis of Type 2 Diabetes Mellitus. *Mol. Cell. Proteomics MCP* **13**, 811–822 (2014).

31. Gómez-Serrano, M. et al. Proteome-wide alterations on adipose tissue from obese patients as age-, diabetes- and gender-specific hallmarks. *Sci. Rep.* **6**, 25756 (2016).
32. Alfadda, A. A., Masood, A., Al-Naami, M. Y., Chaurand, P. & Benabdelkamel, H. A Proteomics Based Approach Reveals Differential Regulation of Visceral Adipose Tissue Proteins between Metabolically Healthy and Unhealthy Obese Patients. *Mol. Cells* **40**, 685–695 (2017).
33. Insenser, M. et al. A nontargeted proteomic approach to the study of visceral and subcutaneous adipose tissue in human obesity. *Mol. Cell. Endocrinol.* **363**, 10–19 (2012).
34. Jt, T. et al. Perilipin ablation results in a lean mouse with aberrant adipocyte lipolysis, enhanced leptin production, and resistance to diet-induced obesity. *Proceedings of the National Academy of Sciences of the United States of America* vol. 98 https://pubmed.ncbi.nlm.nih.gov/11371650/ (2001).
35. Orlicky, D. J. et al. Perilipin-2 promotes obesity and progressive fatty liver disease in mice through mechanistically distinct hepatocyte and extra-hepatocyte actions. *J. Physiol.* **597**, 1565–1584 (2019).
36. Straub, B. K., Stoeffel, P., Heid, H., Zimbelmann, R. & Schirmacher, P. Differential pattern of lipid droplet-associated proteins and de novo perilipin expression in hepatocyte steatogenesis. *Hepatol. Baltim. Md* **47**, 1936–1946 (2008).
37. Murri, M. et al. Proteomic analysis of visceral adipose tissue in pre-obese patients with type 2 diabetes. *Mol. Cell. Endocrinol.* **376**, 99–106 (2013).
38. Shang, C. et al. Comparative Proteomic Analysis of Visceral Adipose Tissue in Morbidly Obese and Normal Weight Chinese Women. *Int. J. Endocrinol.* **2019**, 2302753 (2019).
39. Schöttl, T. et al. Proteomic and Metabolite Profiling Reveals Profound Structural and Metabolic Reorganization of Adipocyte Mitochondria in Obesity. *Obes. Silver Spring Md* **28**, 590–600 (2020).
40. Newgard, C. B. et al. A Branched-Chain Amino Acid-Related Metabolic Signature that Differentiates Obese and Lean Humans and Contributes to Insulin Resistance. *Cell Metab.* **9**, 311–326 (2009).
41. She, P. et al. Obesity-related elevations in plasma leucine are associated with alterations in enzymes involved in branched chain amino acid (BCAA) metabolism. *Am. J. Physiol. Endocrinol. Metab.* **293**, E1552–E1563 (2007).
42. Polyzos, S. A., Kountouras, J. & Mantzoros, C. S. Adipokines in nonalcoholic fatty liver disease. *Metab. - Clin. Exp.* **65**, 1062–1079 (2016).
43. Rochette, J., Craig, J. E., Thein, S. L. & Rochette, J. Fetal hemoglobin levels in adults. *Blood Rev.* **8**, 213–224 (1994).
44. Yuan, X. et al. Proteomic analysis to identify differentially expressed proteins between subjects with metabolic healthy obesity and non-alcoholic fatty liver disease. *J. Proteomics* 103683 (2020) doi:10.1016/j.jprot.2020.103683.
45. Brandtzaeg, P. Transport models for secretory IgA and secretory IgM. *Clin. Exp. Immunol.* **44**, 221–232 (1981).
46. de Marco, M. C. et al. MAL2, a novel raft protein of the MAL family, is an essential component of the machinery for transcytosis in hepatoma HepG2 cells. *J. Cell Biol.* **159**, 37–44 (2002).
47. de Marco, M. C., Puertollano, R., Martínez-Menárguez, J. A. & Alonso, M. A. Dynamics of MAL2 during glycosylphosphatidylinositol-anchored protein transcytotic transport to the apical surface of hepatoma HepG2 cells. *Traffic Cph. Den.* **7**, 61–73 (2006).